

## 12.4

# HAILSTONES, THE MAIN SOURCE OF RAIN

Roland List<sup>1</sup>  
University of Toronto, Toronto, Canada

### 1. INTRODUCTION

The basic elements of the growth of spherical hailstones are defined by their diameter and speed of free fall - as related by the drag coefficient - the cloud liquid water hailstones collect, and their heat and mass transfer. Drag coefficients of smooth spheres have been established by Prandtl (1923) and Bilham and Relf (1937). Neglecting radiative losses, the heat transfer and mass transfer, HMT, through conduction and convection, and evaporation/condensation (sublimation) and the accretion of supercooled cloud water droplets are determining the amount of accreted water that can be frozen. Schumann (1938) produced the first mathematical theory of hail growth with the data available. Ludlam (1958) updated the individual terms and accepted Schumann's (1938) assumption that only water can be accreted that is able to freeze. This is equivalent to saying that all the surplus water is shed. This defines the Schumann-Ludlam Limit, SLL. List (1959a) discovered spongy ice, which consists of a growing ice frame that is stabilizing built-in water. This allows unrestricted growth. The thermodynamics of spongy ice (List, 1960) became the basis for the next theory of hailstone growth by List (1963). With the availability of hail tunnels [List, 1959b, 1966, List et al (1987) and Macklin (19xx)] major facilities became available to study the growth of hailstones under controlled conditions. On the basis of samples of more than 19 hailstorms List established the main shape as ellipsoidal (70%) with axes ratios 1: 0.8: 0.5, and started to study with his group, spheroidal hailstone, as approximations of the ellipsoidal ones. The main aerodynamic discovery was the finding that spheroidal hailstones fall while gyrating about a horizontal axis. [A gyration is composed of a nutation and a 90° phase-shifted precession of the spin axis that moves on the surface of a cone while gyrating. The axes intersection is at the center of the hailstone. Gyration, contrary to rotation, produces relatively smooth accretions without spikes. Nevertheless, gyration and spin can substantially enhance shedding. Lesins and List (1986) identified 5 types. The most interesting mode occurs at high frequencies (> 19 Hz). Such conditions can occur in free fall as Kry and List (1974) postulated and Stewart and List (1983) experimentally confirmed. This shedding initiates and maintains a warm rain process.

This present paper will be laying the foundation for the bold conclusion about the major rain process. In 2007 the author established the free fall mode for

ellipsoidal hailstones (see List and Abreu, 2008). As a side-product the author did a *gedankenexperiment* on the radius-symmetric growth of spheres. The result: spherical hailstones grow while gyrating about a horizontal (gyration) axis while the spin axis is inclined by 45°. Fig. 1 explains the different situations.

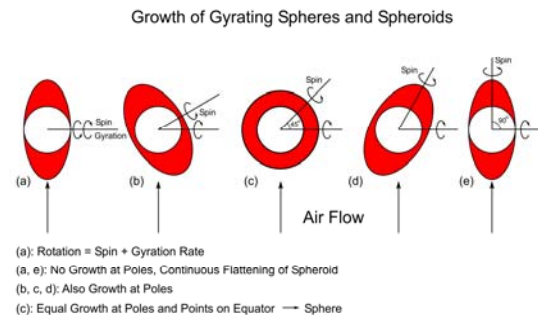


**Fig. 1.** Sphere evolution while gyrating about a horizontal axis, with the spin axis inclined by various angles between 0° and 90° in respect to the horizontal gyration axis. Equal exposure of all surface points occurs when the spin axis is inclined by 45° relative to the gyration axis. Equal exposure means equal growth conditions and equal surface temperatures.

Panel (a) depicts a rotating sphere (with identical gyration and spin axes) which grows only in the fall direction and no growth occurs at the poles. However, as soon as the spin axis rotates about the gyration axis at an angle, growth will also occur at the poles (Panels b, c and d). At a spin axis inclination of 90° (Panel e) the spin axis rotates in a plane perpendicular to the gyration axis. There is no growth in the direction of the (horizontal) gyration axis. Further, the spin has no effect on growth. Panels b and d are describing spheroidal growth. Panel c is the key to spherical growth because the hailstone grows by the same amounts in the direction of the polar axis as in the equatorial plane.

This leads to a major consequence: It the growth is the same at all surface points, then the temperature is also the same at all points. Thus, the development of the physics is much, much easier because no time-consuming, continuous calculations of the internal heat conduction from pole to equator are necessary as performed by Zheng and List (1995). Spherical specimens have been documented by List (1958a) and others. Note that “knobbly” is considered as a description of roughness and not as a basic shape.

<sup>1</sup> Corresponding author address: Roland List, Univ. of Toronto, Dept. of Physics, Toronto, Ontario M5S 1A7; e-mail: roland.list@rogers.com

$$\left[ 0.535 k (t_S - t_A) + 0.511 D_{wa} L_E \frac{(e_S - e_A)}{R_w T_A} \right] \pi K(\tau\theta\kappa) Re^{1/2} D = \left[ -c_w(t_S - t_A) + E_{NC} I_f L_f \right] \frac{\pi}{4} E V D^2 W_f \quad (1)$$

$$K \times \left[ \frac{0.535 k(t_S - t_A) + 0.511 D_{wa} L_{s,e} \frac{1}{R_w T_A} (e_S - e_A)}{0.25 E v L_f [c_w L_f^{-1} (t_S - t_A) - E_{NC} I_f]} \right] \times \sqrt[4]{\frac{3 \rho_A C_D v^2}{4 g \rho_H}} = -W_f D^{3/4} = X \quad (2)$$

## 2. THE HEAT AND MASS TRANSFER (HMT) OF SPHERICAL HAILSTONES

The HMT of hailstones has been treated in many papers [i.e. List (1963), García-García and List (1992), Greenan and List (1995), and Zheng and List (1995)]. It is represented by the sum of the convective and the evaporative parts, and the sensible heat contributed by the accreted water. These heat contributions allow partial or total freezing of the accreted water. Accretion and freezing also have a common multiplication factor as the other two. The first two parts are described by the Nusselt (Nu) and Sherwood (Sh) numbers, respectively, quantities dependent on Reynolds number (Re) and the diameter of the spheres,  $D$ . The HMT terms will be represented by groupings with common factors. Thus, the HMT is given by (1).

The symbols are:  $k$  [ $J m^{-1} s^{-1} \text{ } ^\circ C^{-1}$ ] thermal conductivity of air,  $t_S$  [ $^\circ C$ ] surface temperature,  $t_A$  [ $^\circ C$ ] air temperature,  $D_{wa}$  [ $m^2 s^{-1}$ ] diffusivity of water vapor in air,  $L_E$  [ $J kg^{-1}$ ] latent heat of evaporation,  $e_S$  [Pa] saturation vapor pressure at surface of hailstone,  $e_A$  [Pa] saturation vapor pressure in air,  $R_w$  [ $J kg^{-1} \text{ } ^\circ K^{-1}$ ] Gas Constant for water vapor,  $T_A$  [ $^\circ K$ ] absolute air temperature,  $K(\tau, \theta, \kappa)$  [-] consolidated factor composed of measured effects of roughness, turbulence and gyration,  $Re$  [-] Reynolds number,  $D$  [m] sphere diameter,  $c_w$  [ $J kg^{-1} \text{ } ^\circ C^{-1}$ ] specific heat of water at  $t_A$ ,  $E_{NC}$  [-] net collection efficiency (probability that colliding water droplets are permanently collected),  $I_f$  [-] fraction of permanently accreted water that freezes,  $L_f$  [ $J kg^{-1}$ ] latent heat of fusion,  $E$  [-] collision efficiency,  $V$  [ $m s^{-1}$ ] free fall velocity of spherical hailstone,  $W_f$  [ $kg m^{-3}$ ] liquid water content of air.

Some of the constants in (1) are pressure and temperature dependent. Thus,  $p_A$  will be related to  $t_A$  as Beckwith (1960) did for Denver hailstorms. It is further assumed that  $V$  is coupled to the diameter for appropriate roughness according to List et al (1969). The data show that the flow is supercritical and constant at  $C_D = 0.5$  for  $D \geq 2$  cm up to sizes far beyond  $D = 8$  cm. At lower diameters it increases and  $C_D = 1$  at  $D = 0.5$  cm (List and Schemenauer (1971)).

With these simplifications (1)<sup>1</sup> is consolidated in (2).

Another variable is defined by

$$E_{NC} I_f = Y \quad (3)$$

In replacing  $Re$  by  $D$  [m] for free fall, the kinematic viscosity  $\nu$  [ $m^2 s^{-1}$ ], the drag coefficient  $C_D$  [-], the gravity constant  $g$  [ $m s^{-2}$ ], and the hailstone density  $\rho_H$  [ $kg m^{-3}$ ] have been introduced.

Of the original 8 variables and the constant  $K$ , two other new parameters group, besides  $X$  and  $Y$ , can be defined  $\Phi$  and  $\Psi$ .  $\Phi$  and  $\Psi$  are both functions of temperatures (and pressure) only. The main control of the HMT equation, however, is contained in the two new groups:  $X = W_f D^{3/4}$  and  $Y = E_{NC} I_f$ . Hence (2) can be rewritten in the form of a parabola

$$\frac{\Phi}{Y - \Psi} = X \quad (3)$$

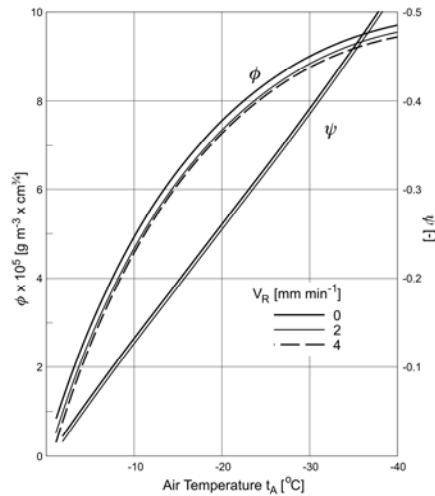


Fig. 2. Air temperature dependence of the parameters  $\Phi$  and  $\Psi$  for  $t_S \approx 0^\circ C$ , with growth rate links.

The values of  $\Phi$  and  $\Psi$  can easily be identified and calculated as functions of  $t_A$  ( $p$ ) and  $t_S$  only. Fig.2 gives their values for  $t_S \approx 0^\circ C$ . The surface

<sup>1</sup> A similar equation had been developed by List and Dussault (1967), but without shedding.

temperature is slightly supercooled for wet/moist growth, depending on the radial speed of growth ( $-0.41^{\circ}\text{C}$  for  $V_R = 2 \text{ mm min}^{-1}$ , and  $-0.52^{\circ}\text{C}$  for  $4 \text{ mm min}^{-1}$ ). Both pairs  $W_f$  and  $D$ , as well as  $E_{NC}$  and  $I_f$ , do not enter the final HMT equation as isolated variables, only their respective products are controlling the final equation. (2) reveals another important point. Both  $C_D$  and the hailstone density  $\rho_H$  enter (2) in the 4<sup>th</sup> root, thus showing insensitivity to these two variables.

### 3. THE CLASSIFICATION OF HAIL GROWTH

#### 3.1. Case 1: Dry growth of hailstones

The purpose of the classification is to achieve a further reduction of variables. The first category deals with the dry growth of hailstones with surface temperatures  $t_s < 0^{\circ}\text{C}$ . This means there is no shedding, and both  $I_f = 0$  and  $Y = 0$ . This leads to a display of surface temperature as function of air temperature (height) and  $W_f$  and  $D$  as represented by  $X$  (Fig. 3). Low values of  $W_f$ ,  $D$ , and low  $t_A$  favor dry growth. The blank area in the lower right side shows where no dry growth is possible. Note that the larger hailstones always grow spongy. Increasing air temperature  $t_A$  also makes it difficult for dry ice to grow.

Two points: (i) The relevant latent heat is that of evaporation from the solid; (ii) the density of deposits on hailstones,  $\rho_H$  could be  $< \rho_{ice}$  – i.e. hailstone growth could be similar to graupel growth<sup>2</sup>. However, this is not likely, and observations of low density outer hailstone shells may have been misinterpreted by not realizing that the water had been drained from spongy ice. Graupel are also examples of overlapping growth stages as they evolve by passing through a densification stage. During this growth phase the porous ice frame is soaked with water, producing ice particles defined as “small hail” with  $D \leq .5 \text{ mm}$ . Subsequent volume growth of small hail leads to hail (List, 1958a and b).

There is another aspect to be considered. Radar observation suggest that 5 cm hailstones should grow from graupel ( $D = 5 \text{ mm}$ ) to 5 cm hail within 10 to 20 min. Mass growth in Section 4 will further address the (low) probability of dry growth of hailstones. An example: For  $W_f = 3 \text{ g m}^{-3}$  hailstones with  $D = 1 \text{ cm}$  grow dry at levels above  $t_A \approx -17^{\circ}\text{C}$ , while 5 cm hailstones always grow spongy.

#### 3.2. Case 2: Spongy growth with heavy shedding,

Mass growth under heavy shedding conditions will always take place at  $t_s \approx 0^{\circ}\text{C}$ . The slight supercooling of the surface is necessary to create a temperature gradient that allows the HMT. It is

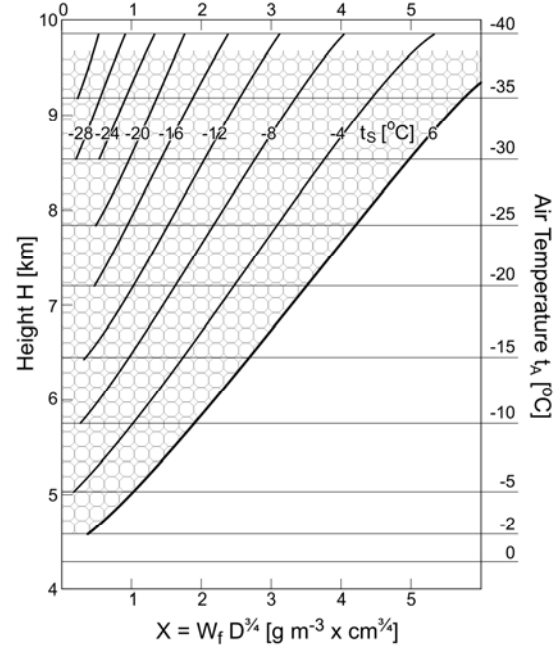


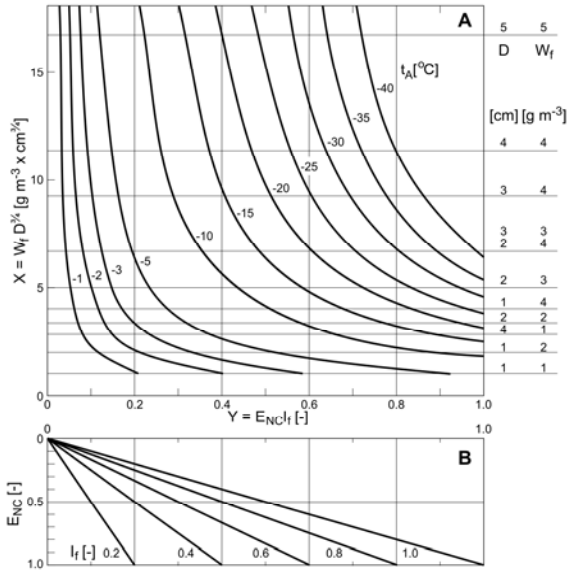
Fig. 3. Dry growth of hailstones in function of  $X (= W_f D^{3/4})$  and height or air temperature, at various surface temperatures  $t_s$ .

dependent on growth speed and will rarely exceed  $0.5^{\circ}\text{C}$ . It will always be accompanied by spongy growth. The relationship between the ice fraction of the net accreted cloud water ( $Y$ ) is displayed in Fig. 4A against  $X$ , the product of  $W_f$  and  $D^{3/4}$  for different  $t_A$ . Higher  $Y$  and larger  $X (= W_f D^{3/4})$  are found at lower  $t_A$ . The situation is reversed when lowering  $X$  and/or  $Y$ . This requires that  $t_A$  moves closer to the freezing point. The upper right corner area represents conditions excluded from the Case 2 scenario because only considerations was given to a limit of supercooling to not more than  $-40^{\circ}\text{C}$ . A Panel B is added with the breakdown of  $Y$  into its components.

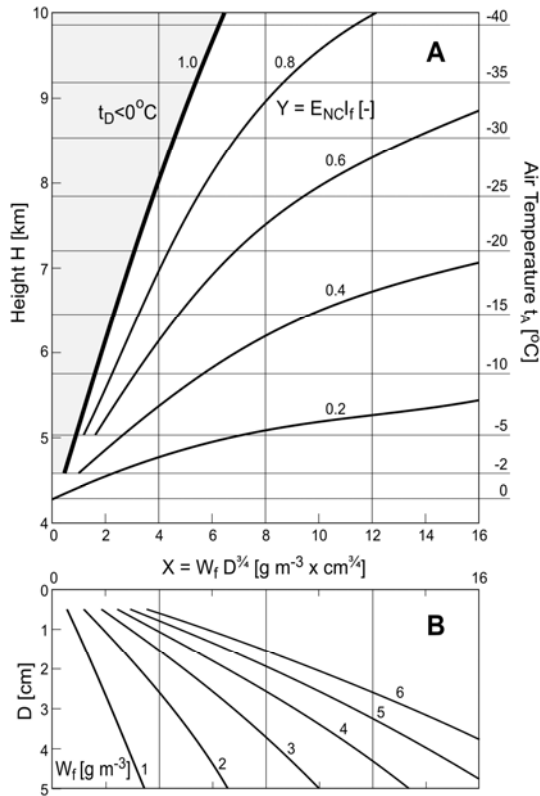
For Case 2 the hailstone is always spongy and the surface moist but without a continuous water skin. Accreted water is always shed before a skin has developed. The surface temperature  $t_s \approx 0^{\circ}\text{C}$ .

Fig. 5 represents the same Case 2 as displayed in Fig. 4 but for a different arrangement of variables. As expected, shedding is favored by higher temperatures. Larger hailstones and larger  $W_f$  always lead to heavier shedding and lower  $Y$ .  $Y = 1$  represents SLL.

<sup>2</sup> The only density measurements of real graupel have been made by List (1958b), with values between  $0.5$  and  $0.7 \text{ g cm}^{-3}$ .



**Fig. 4.** A: The coupling of the parameter groups  $X$  and  $Y$  at different  $t_A$ ; B: breakdown of  $Y$  into the components net collection efficiency  $E_{NC}$  and ice fraction of deposit  $I_f$ .  $Y=1$ : defines the Schumann-Ludlam limit, SLL.



**Fig.5.** Variation of  $Y$  as function of  $X$  and air temperature (Panel A); Panel B showing breakdown of  $X$  into  $W_f$  and  $D$ ; shaded area: excluded from Case 2.

### 3.2. Case 3: Spongy hailstones covered by supercooled water skins

If the gyration/spin frequencies are insufficient to initiate instant shedding of partial water skins on the hailstone surface, then a complete water skin will develop on a spongy hailstone. Plotting the relation  $t_A$  vs  $X$ , with  $Y$  as parameter, gives conditions as depicted in Fig. 3 for surface temperatures  $\approx 0^\circ\text{C}$ . However, since  $t_S$  can also be  $< 0^\circ\text{C}$ , additional conditions similar to Fig. 5 can be calculated. It is suggested that  $t_S$  will be rarely colder than  $-8^\circ\text{C}$ .

This discussion still leaves one question open: the thickness of the water skin. List (1990) theoretically treated the conditions for dendritic ice growing into a supercooled water skin. The equations will not be shown in this present paper. They will be developed in List (2011a and b). However, the results are being displayed in the four panels of Fig. 6. Starting at the right bottom and proceeding counter-clockwise the following information is given: Panel A: Hailstone speed of free fall  $V$  as function of  $t_A$ , for different  $D$ . Panel B: Coupling of the hailstone growth speed with the (radial) growth speed of the ice,  $V_R$ , for different products of  $E_{NC}W_f$ . B further indicates the ice front temperature  $t_o$  ( $V_R$ ). Panel C: relation between the different  $V_R$  and the driving temperature gradient ( $-t_S \sigma^1$ ), for different ice fractions<sup>3</sup>. Panel D: Breaking up the driving temperature gradient into  $t_S$  for various values of  $d$ . The Panels can also be read in reverse direction, except that there is no link between Panel A and D. - The critical factor for this ultimate reduction of variables for Case 3 is the recognition that the radial hailstone growth speed  $V_R$  is equal to the ice front speed.

In general it can be said that, as expected, larger (spherical) hailstones and larger accreted liquid water produce higher ice growth speeds. Higher radial ice growth is connected to higher temperature gradients. The critical thickness of the water skin at which shedding occurs will depend on the overall growth conditions and will have to be determined by experiments on the water skin instability.

## 4. HAILSTONE GROWTH

The above classification and treatment of the different cases does not provide a complete basis for a general overview of hailstone growth. That can only be achieved when the actual growth is assessed. Growth of hailstones is by accretion of cloud water (cloud droplets and/or drops which have been previously shed by other hailstones). At the same time it is diminished by evaporation, which, fortunately, is normally  $< 1\%$ . Thus, only net accretion

<sup>3</sup> Note that  $I_f$  and  $E_{NC}$  are not appearing as a pair.  $E_{NC}$  is coupled to  $W_f$ , while  $I_f$  appears as individual variable.

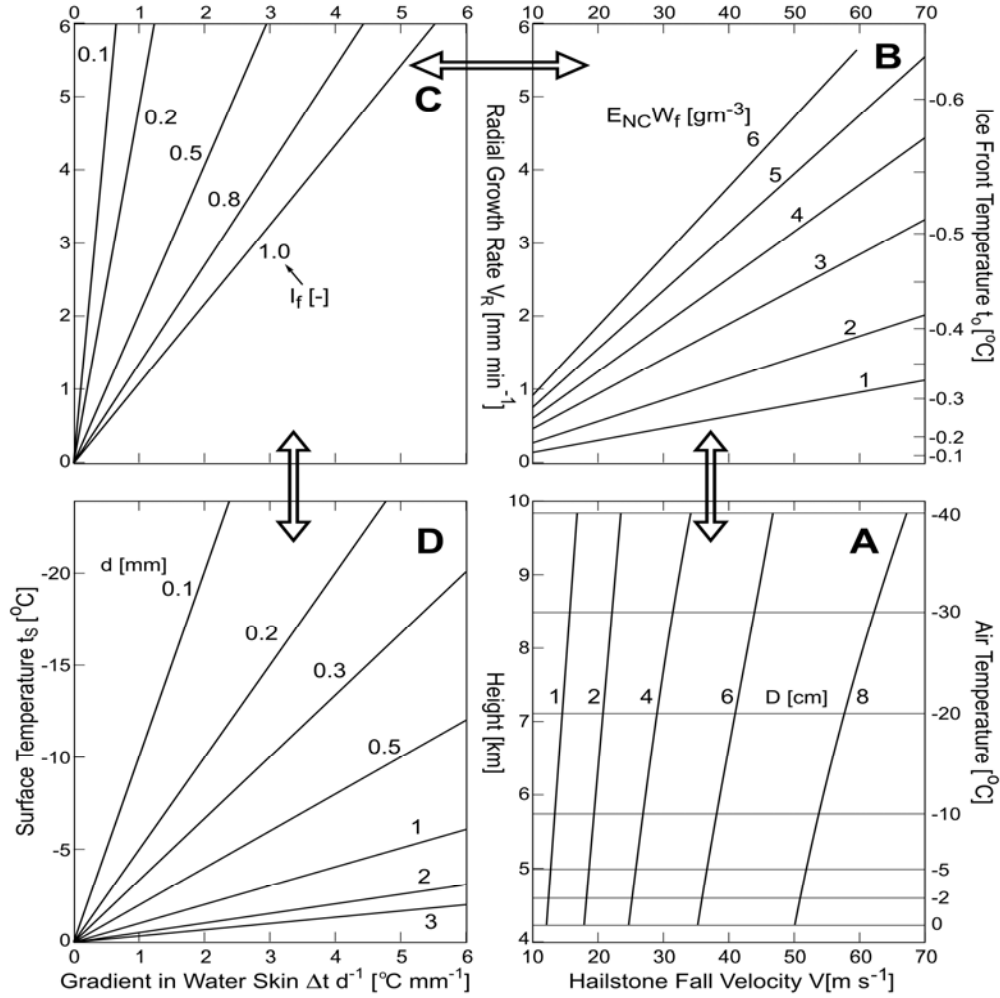


**Fig. 6. A:** Hailstone velocity  $V$  as function of  $t_b$ , at different  $D$ ; **B:** Radial growth speed  $V_R$  and ice front temperature  $t_o$ , as function of  $V$ , at different values of net collected liquid water,  $E_{NC}W_f$ ; **C:** Relation of temperature gradient  $\Delta t/d$  across the water skin in function of hailstone growth speed  $V_R$ , for different values of  $I_f$ ; **D:** Temperature gradient in water skin, as broken down into skin thickness  $d$  and surface temperature  $t_s$ .

is to be considered. As a reminder that shed drops may also be accreted, the collision efficiency  $E$  is carried below, because it may not be equal to unity as is the case for cloud droplets.

The radial growth speed  $V_R$  is half the diameter growth speed  $dD/dt$ . It is proportional to the free fall speed  $V$  ( $\propto D^{1/2}$ ) of the hailstone as well as the accreted liquid water content (4). In colder, thinner air,  $V_R$  increases because it is proportional to  $V$ . Fig. 7 shows the dependence of the radial growth speed from the accreted liquid water content  $EE_{NC}W_f$ , for different diameters at three different temperatures.

$$\frac{dD}{dt} = \frac{1}{2\rho_H} EE_{NC}W_f V \quad (4)$$

Note that the radial growth rate at constant  $EE_{NC}W_f$  increases substantially with hailstone size. This allows large hailstones to grow ‘explosively’ in very short time. Because of this it is not necessary to have updraft speeds in hail clouds that reach values of hailstone fall speeds. At the other end of the size scale it is seen for Case 3 and in combination with Fig. 6, that smaller hailstones have smaller gradients across the water skins and, thus, exhibit less supercooling.

#### 4. SUMMARY AND COMMENTS

The developed hailstone physics covers the full size range of spherical hailstones (diameters 0.5 to 8 cm). The size spectrum starts at the transition from

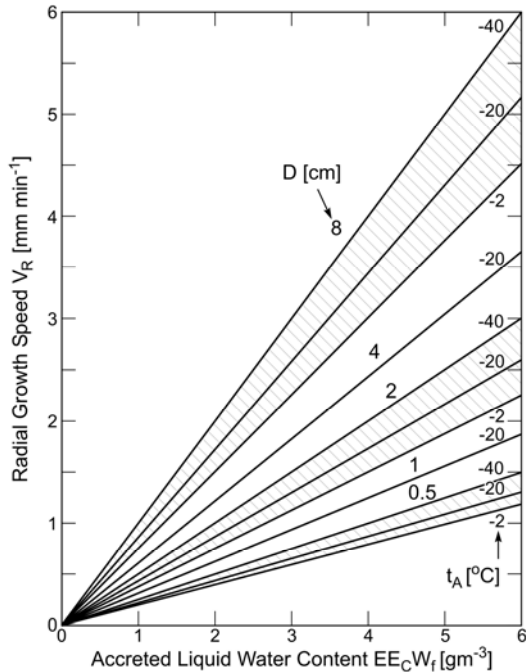


**Fig.7.** Radial growth rate  $V_R$  [ $\text{mm min}^{-1}$ ] as function of the collected and permanently accreted cloud liquid water, for different  $D$  and at  $t_A$  of  $-2$ ,  $-20$ , and  $-40^\circ\text{C}$ .

small hail of 5 mm to hailstones. The upper size limit could have been easily expanded. But from observations 8 cm seems to be a good limit. This may represent the size at which particle inertia brings gyration of spheres to a halt. Indeed, the giant stones collected by Knight and Knight (2005) suggest that the later stages (particles  $>$  than 5 cm ellipsoids) grow without rotational motions [simple etching (see Painter and Schaefer, 1960, and List, 1961) of hailstone cuts could easily verify this].

A new heat and mass transfer, HMT, equation was formulated with the help of 4 new variables for all sizes of freely falling spherical hailstones (range 0.5 to 8 cm) for conditions encountered in hailstorms. Two pairs of products of previous variables, liquid water content and diameter, and net collection efficiency and deposit ice fraction are controlling HMT, while the other two are functions of air and hailstone surface temperature only. A new classification of hail growth into 3 categories contributed to this reduction. They are: Case 1 dry growth; Case 2: fast shedding from spongy hailstones, with moist surfaces and temperatures close to the freezing point; and Case 3: slow shedding from water skin covered spongy hailstones with surface temperatures below the freezing point.

The shed water is like a flow of a coolant over the hailstones, transferring sensible heat from the hailstone to heat the surrounding air. The effect of shedding alone is comparable to the sensible heat term. At  $E_{NC} = 0.5$  the shedding effect is equal to the

cooling by the net accreted water. Decreasing the ice content  $I_f$  in the deposit shifts the balance even more towards the shed water. It needs to be added, however, that lowering the size of the hailstone makes the sensible heat term less important compared to the conduction/convection and evaporation terms,

For small 5-10 mm hailstone sizes, presently with relatively high errors, the HMT could easily be refined to reduce the errors from the present  $< \pm 25\%$ .

Hailstones can grow larger when they spend more time in a favorable growth environment. This occurs when they do not scavenge all liquid cloud water, and the shed water is later available for further hail growth (and for a parallel rain process). Many scenarios are possible with multi-type particles competing with each other (Joe, 1982; Joe and List, 1984; Joe et al 1980; or as shown by List et al, 1968). Shed drops could also initiate a new hail generation by freezing. This is not considered to be a major factor since supercooling is often the rule, particularly when all the ice nuclei have been scavenged before (not well known by non-experimentalists). [Injecting tap water into the hail tunnel the author has observed regular supercooling of injected tap-water droplets with diameters of 20 to 40  $\mu\text{m}$  down to  $-34^\circ\text{C}$ . On the other hand injection of AgI smoke led to a transition of growth of palisade-like, radially arranged ice single crystals in deposits to a structure consisting of small crystals (List, 1961)]. Thus, the onset of freezing has to be left to the scenario chosen by the modeler. The author also notes that in his many years of icing tunnel experiments he has never seen ice splinters/crystals except when they were purposely injected (Berdeklis and List, 1992). Their scintillations make them easily visible.

A question arises about the difference of heavy shedding from moist hailstones (Case 2) and the shedding from water skin-covered hailstones (Case 3). The answer is simple: the heat and mass transfer from water skin-covered hailstones is reduced when compared to moist hailstones because their surface temperatures are not  $\approx 0^\circ\text{C}$ , they are colder and, thus, produce lower surface to air gradients.

Shedding is circumventing the bottleneck of cloud droplet to raindrop evolution from 50 to 100  $\mu\text{m}$ , because the shed drops have diameters of  $\sim 1.2$  mm (Joe, 1982, 1984; Joe et al, 1980). The original properties of the cloud droplets are lost in the shed drops, considering that it takes 216 000 20  $\mu\text{m}$  cloud droplets to form one shed drop.

It has been shown that the two main hail growth processes involve shedding of water drops (Cases 2 and 3). This provides strong support to the notion that hailstone growth triggers instant transformation of cloud water into rain. Shedding as a major rain formation process, has been experienced in Malaysia and Indonesia where decent rain only occurs in the

presence of the ice phase in the clouds. Ice means graupel, means at least small hailstones. Unfortunately, the ratio between warm and cold rain amounts for the Amazon basin and other parts of the world is unknown.

*A world of caution: There are no modern cloud models available that reflect real hail clouds with particle packaging as observed by Thomson and List (1993), and discussed in List (2010). Those high resolution (100 x 100 x 100 m) Doppler radar observations suggest that there is no smooth airflow in thunderstorms as is normally depicted in textbooks. There are no continuous, nearly steady state "conveyor belts" to move growing hailstones through a storm! Updrafts form a violent environment, as is expected from the behavior of plumes and thermals. How is large scale turbulence evolving and how can it be described? There is no point to apply the conclusions of this paper and List (2011a and b) into staid and "old hat", unrealistic dynamic cloud models.*

It is suggested that when the development of new dynamic models of clouds is moving to a front burner, then the warm rain process reflected in the evolution of the shed water could be modeled with the pressure adapted collision, coalescence and breakup work, as developed on the basis of experiments by List, Fung and Nissen (2009) and the para-meterization by List, Nissen and Fung (2009).

The physics presented in this paper may not be the ultimate answer. While many of the steps are based not just on theory but also on experiment, they do not present proof enough. That has to be provided by icing wind tunnel experiments, with gyrations producing spherical hailstones. Such experiments could provide further details of the shedding conditions and modify the results. (Another weakness is the lack of full understanding of gyration motions and their dependence on particle diameter.)

The hailstone physics developed in this paper and List (2011a and b) does not categorically forbid the existence of (smaller) "dry" hailstones. But the lack of a convincing and well supported proof of their existence is noted. Summarizing the evidence, a strong statement is appropriate: **Hailstones generally do not grow dry, they mostly grow beyond the Schumann-Ludlam limit, i.e. they have moist or water skin-covered surfaces and exhibit various degrees of sponginess. Their growth is accompanied by shedding, which may initiate and sustain the most important rain mechanism.**

#### **Acknowledgements.**

The author appreciates the encouragement of this work by Dr. Andrew Heymsfield and Dr. Roy Rasmussen. Unfortunately their work on shedding had not been referred to (Rasmussen and Heymsfield, 1987a, b, and c). These papers with the issue of hailstone embryos and density will be addressed in

List (2011a and b). - The University of Toronto provided a stimulating environment. The Roland List Foundation is to be thanked for full financial support.

#### **REFERENCES**

Beckwith, W. B., 1960: Analysis of hailstorms in the Devnver network, 1949-1958. *Physics of Precipitation. Geophys. Monogr.*, No. 5, Amer. Geophys. Union, 348-358.

Berdeklis, P., and R. List, 2001: The ice crystal-graupel collision charging mechanism of thunderstorm electrification. *J. Atmos. Sci.*, **58**, 2751-2770.

Bilham, E. G., and E. F. Relf, 1937: The dynamics of large hailstones, *Quart. J. Roy. Meteor. Soc.*, **62**, 149-162.

Frössling, N., 1938: Über die Verdunstung fallender Tropfen. *Beitr. Geophys.* **52**, 170 – 216.

Garcia-Garcia, F., and R. List, 1992: Laboratory measurements and parameterizations of supercooled water skin temperatures and bulk properties of gyrating hailstones. *J. Atmos. Sci.* **49**, 2058-2073.

Greenan, B.J.W., and R. List, 1995: Experimental closure of the heat and mass transfer theory of spheroidal hailstones, *J. Atmos. Sci.*, **52**, 3797-3815.

Joe, P., 1982: The shedding of millimeter sized raindrops in simulated hail formation, PhD thesis, University of Toronto, pp. 306.

Joe, P. J., R. List and G.B. Lesins, 1980: Ice accretions, part II: Rain production by icing assisted cloud water conversion. *J. Recherches Atmos.* **14**, 3-4, 356-364.

Joe, P., and R. List, 1984: Numerical modeling of hail to rain conversion. *Proceedings, Ninth International Cloud Physics Conference*, Tallinn, USSR, 21-28 August, Vol. I, 261-263.

Knight, C. A., and N. C. Knight, 2005: Very large hail: Growth conditions and falling behavior. *Bull. Amer. Meteor. Soc.*, **86**, 1773-1881

Kry, P. R., and R. List, 1974: Angular motions of freely falling spheroidal hailstone models, *Phys. Fluids*, **17**, No. 6, 1093-1102.

Lesins, G.B., and R. List, 1986: Sponginess and drop shedding of gyrating hailstones in a pressure-controlled wind tunnel. *J. Atmos. Sci.*, **43**, 1 Dec., 2813-2825.

List, R., 2011a: Advanced hailstone physics, Pt. I: Classification and heat and mass transfer. *J. Atmos. Sci.*, **49**, to be submitted.

- List, R., 2011b: Advanced hailstone physics, Pt. I: Case studies and growth. *J. Atmos. Sci.*, **68**, to be submitted.
- List, R., 2010: Challenging cloud physicists. 13<sup>th</sup> AMS Cloud Physics Conference, Portland OR, June 28-July 2, P1.83, pp 7.
- List, R., 1990: Physics of supercooling of thin water skins covering rotating hailstones. *J. Atmos. Sci.*, **68**, 1919-1925.
- List, R., 1966: A hail tunnel with pressure control. *J. Atmos. Sci.*, **23**, No. 1, 61-66.
- List, R., 1963: General heat and mass exchange of spherical hailstones. *J. Atmos. Sci.*, **20**, No. 3, 189-197.
- List, R., 1961: Physical methods and instruments for characterizing hailstones. *Bull. Amer. Met. Soc.*, **42**, 452-466.
- List, R., 1960a: Zur Thermodynamik teilweise wässriger Hagelkörner. *Z. angew. Math. Phys.*, **11**, No. 4, 273-306.
- List, R., 1960b: Design and operation of the Swiss hail tunnel. *Phys. Precip., Geophys. Monograph No. 5*, Amer. Geophys. U., Baltimore, 310-316.
- List, R., 1959a: Wachstum von Eis-Wassergemischen im Hagelversuchskanal. *Helv. Phys. Acta.*, **32**, No. 4, 293-296.
- List, R., 1959b: Der Hagelversuchskanal. *Z. angew. Math. Phys.*, **10**, No. 4, 381-415.
- List, R., 1958a: Kennzeichen atmosphärischer Eisparkeln, 1. Teil. *Z. angew. Math. Phys.*, **9a**, No. 2, 180-192.
- List, R., 1958b: Kennzeichen atmosphärischer Eisparkeln, 2 Teil. *Z. angew. Math. Phys.*, **9a**, No. 3, 217-234.
- List, R., and J.-G. Dussault, 1967: Quasi steady state icing and melting conditions and heat and mass transfer of spherical and spheroidal hailstones. *J. Atmos. Sci.*, **24**, No. 5, 522-529.
- List, R., and R.S. Schemenauer, 1971: Free fall behaviour of planar snow crystals, conical graupel and small hail. *J. Atmos. Sci.*, **28**, No. 1, 110-115.
- List, R., C. Fung and R. Nissen, 2009: Experiments on the pressure effect on collision and breakup of raindrops. *J. Atmos. Sci.*, **66**. No.8, 2190-2203
- List, R., R. Nissen and C. Fung, 2009: The parameterization and propagation of pressure effects on raindrop interactions in rainshafts. *J. Atmos. Sci.*, **66**, No. 8, 2204-2215.
- List, R., G.B. Lesins, F. Garcia-Garcia and D.B. McDonald, 1987: Pressurized icing tunnel for graupel, hail and secondary raindrop production. *J. Atmos. Ocean. Techn.*, **4**, No. 3, 454-463.
- List, R., U.W. Rentsch, P.H. Schuepp and N.W. McBurney, 1969: The effect of surface roughness on the convective heat and mass transfer of freely falling hailstones. *Proc. Sixth Conf. Severe Local Storms*, Chicago, Ill., 267-269.
- List, R., R.B. Charlton and P.I. Buttus, 1968: A numerical experiment on the growth and feedback mechanisms of hailstones in a one-dimensional steady state model cloud. *J. Atmos. Sci.*, **25**, No. 6, 1061-1074.
- Ludlam, F. H., 1958: The hail problem. *Nubila*, **1**, 12-99.
- Painter, P. R., and V. J. Schaefer, 1960: Permanent replicas of the crystalline structure of hailstones, *Z. angew. Math. Phys.*, **11**, 318-326.
- Prandtl, L., 1923: Versuche über den Luftwiderstand gerundeter und kantiger Körper; *Ergebn. aerodyn. Vers. Anstalt, Göttingen*, **2**, 29-32.
- Rasmussen, R. M., and A.J. Heymsfield, 1987a: Melting and shedding of graupel and hail. Part 1: Model Physics. *J. Atmos. Sci.*, **44**, 2754-2763.
- Rasmussen, R. M., and A.J. Heymsfield, 1987b: Melting and shedding of graupel and hail. Part 2: Sensitivity Study. *J. Atmos. Sci.*, **44**, 2764-2782.
- Rasmussen, R. M., and A.J. Heymsfield, 1987c: Melting and shedding of graupel and hail. Part 3: Investigation of the role of shed drops as hail embryos in the 1 August CCOPE Severe Storm. *J. Atmos. Sci.*, **44**, 2783-2803.
- Schumann, T. E. W., 1938: The theory of hailstone formation. *Quart. J. Roy. Meteor. Soc.*, **64**, 3-21.
- Stewart, R.E., and R. List, 1983: Gyration motions of disks during free fall. *Phys. Fluids*, **26**, 920-927.
- Thomson, A.D., and R. List, 1998: High resolution measurement of a hail region by vertically pointing Doppler radar. *J. Atmos. Sci.*, **56**, 2132-2151.
- Zheng Guoguang and R. List, 1995: Convective heat transfer of rotating spheres and spheroids with non uniform surface temperatures. *Intern. J. Heat Mass Transfer*, **39**, 1815-1826